

The Neurofibromatosis Type 2 Gene Product, merlin, Reverses the F-Actin Cytoskeletal Defects in Primary Human Schwannoma Cells

Anne-Marie Bashour,¹ J.-J. Meng,¹ Wallace Ip,¹ Mia MacCollin,² and Nancy Ratner^{1*}

Department of Cell Biology, Neurobiology and Anatomy, University of Cincinnati College of Medicine, Cincinnati, Ohio 45267,¹ and Neurology Unit, Massachusetts General Hospital East, Charlestown, Massachusetts 02129²

Received 13 June 2001/Returned for modification 20 August 2001/Accepted 2 November 2001

Schwannoma tumors, which occur sporadically and in patients with neurofibromatosis, account for 8% of intracranial tumors and can only be treated by surgical removal. Most schwannomas have biallelic mutations in the *NF2* tumor suppressor gene. We previously showed that schwannoma-derived Schwann cells exhibit membrane ruffling and aberrant cell spreading when plated onto laminin, indicative of fundamental F-actin cytoskeletal defects. Here we expand these observations to a large group of sporadic and *NF2*-related tumors and extend them to schwannomatosis-derived tumors. Mutation at *NF2* correlated with F-actin abnormalities, but the extent of morphological change did not correlate with the type of *NF2* mutation. We used a recently described molecular strategy, TAT-mediated protein transfer, to acutely introduce the *NF2* protein, merlin, into primary human schwannoma cells in an attempt to reverse the cytoskeletal phenotype. Abnormal ruffling and cell spreading by cells with identified *NF2* mutations were rapidly reversed by introduction of TAT-merlin. The effect is specific to TAT-merlin isoform 1, the growth-suppressive isoform of merlin. TAT-merlin isoform 2, a TAT-merlin mutant (L64P), and merlin lacking TAT were ineffective in reversing the cytoskeletal phenotype. Results show that merlin isoform 1 is sufficient to restore normal actin organization in *NF2*-deficient human tumor cells, demonstrating a key role for merlin in the *NF2* phenotype. These results lay the foundation for epigenetic complementation studies in *NF2* mouse models and possibly for experiments to evaluate the utility of merlin transduction into patients as protein therapy.

Schwannomas are benign encapsulated Schwann cell tumors that occur sporadically and in patients with the diseases neurofibromatosis type 2 (*NF2*) and schwannomatosis. *NF2* patients uniformly develop schwannomas on the vestibular portion of the eighth cranial nerve and often on other cranial nerves, spinal roots, or peripheral nerves. The *NF2* gene on human chromosome 22q12 was cloned (36, 47), enabling mutational analysis of patient blood samples and “second-hit” analysis of *NF2*-related tumors. Most *NF2* patient tumors and sporadic schwannomas have biallelic inactivating mutations in the *NF2* gene (3, 8, 25, 31, 37), consistent with its action as a tumor suppressor. Schwannomatosis patients do not carry *NF2* germ line mutations, and the molecular basis of their disease remains unknown, yet schwannomas from schwannomatosis patients also have biallelic *NF2* mutations (19). We hypothesized that all three classes of schwannoma have cellular changes resulting from *NF2* inactivation and would respond to similar therapeutic approaches.

How *NF2* functions as a tumor suppressor is being intensively studied. The type and location of mutations do not predict schwannoma cell proliferation (18). Schwannoma cells express the Schwann cell marker proteins S100 and vimentin and often the intermediate filament protein GFAP (20, 21) and usually grow slowly in vitro (16, 32, 35).

The *NF2* protein, merlin or schwannomin, belongs to the

ERM (ezrin-moesin-radixin) family of membrane-cytoskeleton linking proteins. ERM proteins have N-terminal halves that interact with membrane proteins and a C-terminal region that mediates binding to the actin cytoskeleton (2). Merlin lacks the C-terminal actin-binding site common to ERM proteins but binds actin via its N-terminal domain (6, 48). Merlin also interacts with the cytoskeleton indirectly through ERM proteins (11, 15, 24, 27, 29). If merlin regulates the actin cytoskeleton, loss of *NF2* in schwannomas is expected to cause tumor formation through disruption of cell shape, cell matrix, and cell-cell communication or signaling functions attributed to actin-plasma membrane interactions.

Comparison of primary normal human Schwann cells (NHSCs) and cells isolated from schwannomas (32) revealed striking differences between the two cell types. Schwannoma cells had five- to sevenfold-larger surface areas and actin-rich membrane ruffles on contact with laminin that were absent in NHSCs. The actin cytoskeletal changes could not be linked to the *NF2* mutation because genetic information on the tumors analyzed was unavailable.

If these cytoskeletal abnormalities are due to the absence of merlin, then introduction of merlin into these cells should rescue the aberrant cytoskeletal phenotype. To carry out quantitative experiments on the very small numbers of primary human schwannoma cells available, and since human Schwann cells are largely resistant to transfection and retroviral infection (16), we used the technique of TAT protein transduction pioneered by Nagahara et al. (28). When added to culture medium, TAT proteins enter cells in a concentration-dependent manner and are refolded, presumably by endogenous

* Corresponding author. Mailing address: Department of Cell Biology, Neurobiology and Anatomy, University of Cincinnati College of Medicine, 3125 Eden Ave., Cincinnati, OH 45267. Phone: (513) 558-6079. Fax: (513) 558-4454. E-mail: nancy.ratner@uc.edu.

chaperones (28, 40). Using this technique, we generated merlin fusion proteins containing an 11-amino-acid NH_2 -terminal domain from the human immunodeficiency virus (HIV) TAT protein. Here we present evidence that merlin isoform 1 reverses the abnormal cytoskeletal phenotypes of schwannoma cells from tumors that occurred sporadically or in NF2 or schwannomatosis patients.

MATERIALS AND METHODS

Patient information. Patient diagnosis was based on clinical criteria (12, 19). Tissues from clinically indicated procedures were collected after pathological examination. Tumors were divided at surgery, with half snap frozen and half placed into tissue culture medium. Tumor NF2-8 and paired normal liver tissue were collected at autopsy. DNA was extracted from peripheral blood leukocytes using the Puregene DNA extraction kit (Gentra Systems) and from frozen pulverized tumor tissue by sodium dodecyl sulfate-proteinase K digestion followed by phenol-chloroform extraction.

Genetic analysis of tumor specimens. We amplified the first 15 *NF2* exons from genomic tumor DNA and separated products on nondenaturing polyacrylamide gels to identify single-strand conformational polymorphisms (SSCP) (19). Comparison with known controls allowed identification of aberrant mobility. Sequencing determined the molecular basis for each aberration. SSCP and sequencing of genomic DNA from peripheral blood specimens were limited to exons with alterations in paired tumor specimen. Loss-of-heterozygosity analysis used primer pairs from polymorphic microsatellite markers proximal to *NF2* (D22S275 and D22S193), distal to *NF2* (D22S268 and D22S430), and intragenic markers (D22S929 and NF2TET) (19). We analyzed all blood tumor pairs with a minimum of two informative markers.

Cell culture. Normal human nerves were bathed for 5 days in Dulbecco's modified Eagle's medium (DMEM)–10% fetal bovine serum (FBS)–penicillin–streptomycin (Gibco)–2 μM forskolin (Calbiochem)–14 ng of recombinant human glial growth factor (rhGGF2) per ml (23). Medium was changed every two days. Tumors were dissociated immediately on receipt in the lab. Nerve and tumor dissociation was done for 4 to 6 h at 37°C in 20 ml of L15 medium (Gibco) with 1.25 U of dispase (Boehringer-Mannheim) per ml, 0.05% collagenase (Worthington Biochemicals), and gentamicin (50 $\mu\text{g}/\text{ml}$). Samples were centrifuged, and pellets were resuspended in serum-free N2 medium with 2 μM forskolin plus 14 ng of rhGGF and 50 μg of gentamicin per ml (growth medium) and then plated onto poly-L-lysine-coated dishes (32). To avoid cell loss, tumor cells were plated in 100 μl of growth medium for 10 min, and then 1.5 ml of growth medium was added. Typical tumor specimens resulted in sufficient cells for plating in a single 35-mm dish.

Expression and purification of TAT-merlin. We used primer-based PCR to tag the human cDNAs encoding merlin isoforms 1 and 2 with a human c-Myc epitope (24) and inserted them into the *EcoRI* site of pTAT (28), producing pmTAT-NF2-1 and pmTAT-NF2-2, respectively. Mutant merlin (L64P), found in some NF2 patients and segregating with disease (<http://neurosurgery.mgh.harvard.edu/NFresrch.htm>), was generated using the Quick Change mutagenesis kit (Stratagene). Sequencing confirmed the fidelity of PCR amplification and in-frame ligation.

Bacterial clones of BL21(DE3) transformed with pTAT-NF2-1 or pTAT-NF2-2 were cultured in Luria-Bertani broth to an optical density at 280 nm of 0.5 to 0.6. Isopropyl-1-thio- β -D-galactopyranoside (IPTG) was then added to 0.4 mM. After 3 to 5 h of shaking at low speed, cells were pelleted at $3,000 \times g$ and then suspended in lysis buffer (300 mM NaCl, 50 mM Tris-HCl [pH 8.0], 0.1% Triton X-100). After 0.5 mM phenylmethylsulfonyl fluoride and 100 μg of lysozyme per ml addition, the cell suspension was placed on ice for 20 min, ultrasonicated, and then clarified by centrifugation at $12,000 \times g$ for 10 min. The supernatant contained native TAT-merlin that was further purified using Nitrotriacetic acid column and a desalting PD-10 column (28). Protein concentration was measured with a BCA kit (Pierce).

Ruffling assays. Purified TAT protein was added to the N2 medium bathing schwannoma cells for 5 h. The cells were then washed and trypsinized, and 5×10^3 to 10×10^3 cells were plated onto laminin-coated cover slips as a 20- μl drop in N2 medium (32). Fifteen minutes later, wells were flooded with N2 plus 10% FBS for 30 min, and then cells fixed in 4% paraformaldehyde for 10 min. To identify Schwann cells, we stained with anti-rabbit S100 β antibody (1:6,000, Dako) followed by tetramethyl rhodamine isocyanate (TRITC)-conjugated goat anti-rabbit immunoglobulin G (IgG) (Jackson Labs) and 4,4'-difluoro-3a,4a-diaza-5-indacene BODIPY Fluor or Alexa Fluor 488 phalloidin (Molecular

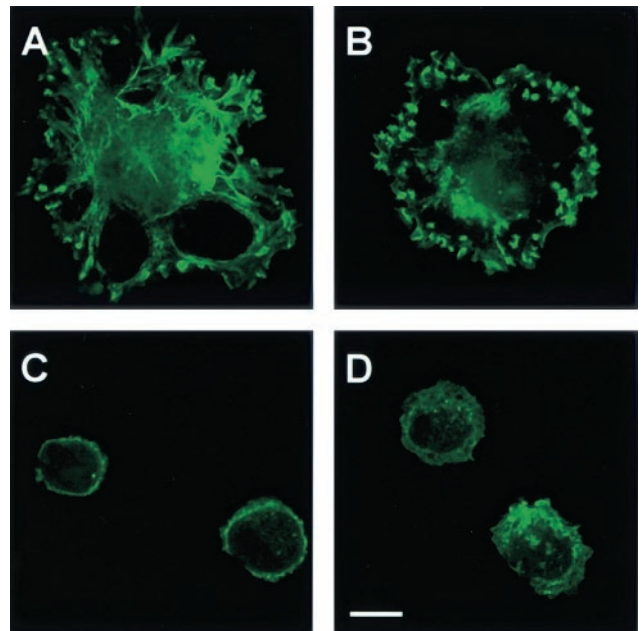


FIG. 1. Abnormal F-actin organization in schwannoma and schwannomatosis cells. Cells were plated onto laminin-coated coverslips, serum was added, and cells were fixed and stained with BODIPY-phalloidin to visualize F-actin (A to D) and then analyzed by confocal microscopy. Membrane ruffles are present on cells from a sporadic schwannoma (A) and a schwannoma from a schwannomatosis patient (B) but not normal human Schwann cells (C) or neurofibromatosis type 1 neurofibroma-derived Schwann cells (D). Bar, 10 μm .

Probes) for visualizing microfilaments. Monoclonal anti-Myc antibody 9E10 was used to visualize TAT-merlin. Cells were viewed and photographed on a Zeiss LSM510. Percent membrane ruffling was calculated as the number of S100-positive Schwann cells exhibiting ruffles divided by the total number of Schwann cells counted. For each sample, at least 100 Schwann cells were counted.

Perimeter measurements. Five thousand cells were plated on laminin-coated cover slips, allowed to adhere for 15 min, and then incubated in N2 plus 10% FBS for 3 h. Cells were fixed and stained as described above. For each sample, the perimeters of 20 cells were traced, and areas were calculated using Meta-morph software (Universal Imaging).

RESULTS

Schwannoma cells have abnormal actin organization. To characterize the schwannoma cell actin cytoskeleton, the F-actin staining patterns of normal human Schwann cells and schwannoma cells were analyzed. Confirming Pelton et al. (32), Schwann cells from sporadic schwannomas (Fig. 1A) and NF2 patient schwannomas (Table 1) showed ruffling plasma membranes 30 min after plating onto laminin. To determine if schwannoma cells from schwannomatosis patients also exhibit ruffling, cells were analyzed as above. Cells from schwannomatosis patients showed intense membrane ruffling (Fig. 1B). In contrast, no cells with ruffling membranes were detected in preparations of normal human (Fig. 1C) or neurofibroma Schwann cells (Fig. 1D). In addition, the spread area was measured on 20 S100-positive cells from each sample. Normal human Schwann cells and Schwann cells from neurofibroma tumors exhibited areas of less than 3,000 μm^2 , whereas schwannoma and schwannomatosis cells had areas ranging from 1,000 to 10,000 μm^2 (Table 1). Thus, abnormal actin

TABLE 1. Schwann cells isolated from patients with NF2 or sporadic or schwannomatosis tumors exhibit membrane ruffling and increased spread area^a

Cell source and sample no.	% of cells with ruffling membranes	No. of cells with designated area (1,000 μm^2)			% of cells with area >3,000 μm^2
		0-3	3-6	>6	
NHSC5					
1	0	20	0	0	0
2	0	20	0	0	0
3	0	20	0	0	0
4	0	20	0	0	0
5	0	20	0	0	0
NF1					
1	0	20	0	0	0
2	0	20	0	0	0
3	0	20	0	0	0
NF2					
1	37 (35)	4	15	1	80
2	50 (43)	5	11	4	75 (60)
3	15	1	13	6	95
4	59	17	3	0	15
5	97	3	5	2	35
6	90	0	3	17	100
7	46	3	11	6	85
8	40	13	7	0	35
9	97	6	14	0	70
Schwannomatosis					
1	35 (33)	18	2	0	10
2	49 (50)	4	2	14	80 (60)
3	26	7	7	6	65
4	35	14	6	0	30
5	27		n.d.		n.d.
Sporadic schwannoma					
1	22 (29)	8	6	6	60 (60)
2	21		n.d.		n.d.
3	20		n.d.		n.d.
4	31		n.d.		n.d.
5	96		n.d.		n.d.
6	99		n.d.		n.d.
7	61	9	11	0	55

^a Membrane ruffling and cell spreading assays were performed on cells isolated from designated tumor samples at passage 0. Some tumor strains were reassayed for membrane ruffles or cell spreading at passage 1. Reassay data are shown in parentheses. n.d., not done.

phenotypes are present in cells from each schwannoma, be it sporadic or from NF2 or schwannomatosis patients.

However, not every schwannoma cell exhibited actin abnormalities. The percentage of cells with ruffling membranes and the percentage of cells with a spread area greater than 3,000 μm^2 within each preparation are shown in Table 1. The percentage of the S100-positive cells showing ruffling varied from a low of 15% to a high of 97%. Cells from several tumors were assayed over two sequential passages and showed similar numbers of cells with increased size at each passage (Table 1). The differences among cells in a specific sample are therefore unlikely to have been caused by passage effects or by day-to-day variation in assay conditions.

Genetic analysis of tumor and blood specimens. A possible explanation for variability in the percentage of cells showing aberrant actin cytoskeleton within an individual tumor is that specific *NF2* mutations influence the extent of ruffling and cell spreading. To determine whether variability in the percentage

TABLE 2. *NF2* locus analysis^a

Sample no.	Exon	Sequence change	Result	LOH
NF2-1	15	1646 del 1 BP (T)	Frameshift	Yes
NF2-2	UF			No
NF2-3	6	G552A, Trp184X	Nonsense	No
	5	C465T, Pro155Pro	PM	
	5	C459G, Tyr153X	Nonsense	
NF2-4	n.d.			n.d.
NF2-5**	5	C459A, Tyr153X	Nonsense	No
NF2-6**	5	C459A, Tyr153X	Nonsense	Yes
NF2-7	12	1199 del 2 bp (AG)	Frameshift	No
NF2-8	11	C1021T, Arg341X*	Nonsense	Yes*
NF2-9	1	C111A	Nonsense	No
Sch-1	7	630 ins 1 bp (T)	Frameshift	Yes
Sch-2	UF			Yes
Sch-3	6	g599+4a	PM	Yes
	15	1594 del 1 BP (A)	Frameshift	
Sch-4	n.d.			n.d.
Sch-5	n.d.			n.d.

^a Mutations are listed in the format given in Jacoby et al. (19), with the numbering of bases showing alterations relative to the cDNA sequence with the initiator ATG beginning at base 1. Alterations seen in the paired blood sample are printed in bold. *, liver specimen used instead of paired blood sample. UF, no mutation detected by exon scanning. PM, putative polymorphism. LOH, loss of heterozygosity. **, the NF2-5 and NF2-6 tumors were two anatomically distinct spinal cord tumors from the same patient. n.d., not determined.

of cells with ruffling correlates with a specific type of *NF2* mutation, genetic analysis was performed on tumors from eight NF2 patients and three schwannomatosis patients. Typical mutations were detected in the *NF2* gene in 9 of 11 tumors studied (Table 2). In six of eight tumors from NF2 patients, the mutation detected was also present in the corresponding blood sample, indicating that it was the germ line mutation causing the patient's NF2. None of the mutations detected in tumors from schwannomatosis patients were detected in the blood sample, consistent with previous results showing lack of germ line *NF2* mutation in these patients (19).

Unexpectedly, putative polymorphisms were detected in two samples. In sample NF2-3, a C to T transition at a codon wobble position in exon 5 was seen in both tumor and paired blood specimens. Because a typical germ line mutation was also detected in this patient, it is unlikely that this silent change contributes to the patient's phenotype. In patient SCH-3, an intronic change was detected at a nonconserved position 4 bp 3' to exon 6. This alteration was seen in the patient's blood sample and the sample from the patient's father, who was unaffected, suggesting that it is a benign polymorphism.

Second hits were detected in 7 of 12 tumors studied. In a single case (NF2-3), a second mutation was detected in the tumor and not found in the blood sample. In six other tumors, loss of heterozygosity of flanking and/or intragenic markers was seen in the tumor specimen relative to the blood. In all cases, loss or retention was seen with all informative markers studied, as expected. The data are consistent with loss of *NF2* function in schwannoma cells, but the extent of the F-actin cytoskeletal abnormalities did not correlate with the type of *NF2* mutation.

TAT-linked merlin protein enters schwannoma cells. To test the feasibility of using TAT-linked proteins to transduce cells, TAT-merlin protein with a C-terminal Myc tag was generated (Fig. 2A and B). Normal human Schwann cells in culture

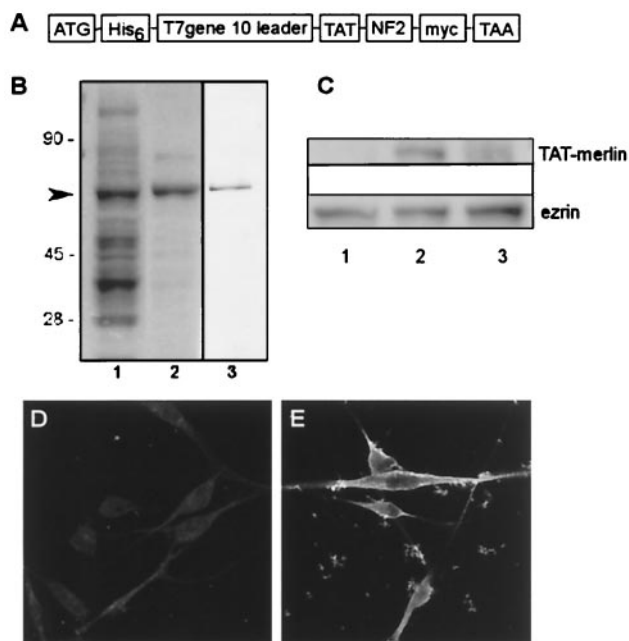


FIG. 2. Purification and analysis of TAT-merlin. (A) Schematic of TAT-merlin constructs. (B) Coomassie blue-stained gel showing bacterial extract expressing TAT-merlin (lane 1) and purified TAT-merlin (6 µg) (lane 2). Lane 3 shows a Western blot of lane 2 stained with anti-merlin antibody. (C) Normal human Schwann cells were untreated (lane 1), treated with TAT-merlin isoform 1 for 5 h (lane 2), or treated for 5 h followed by 16 h without TAT-merlin (lane 3). Western blots of cell lysates were probed with anti-Myc. Control schwannoma cells (D) and schwannoma cells incubated with 100 µg of TAT-merlin isoform 1 per ml for 5 h (E) were fixed and then stained with anti-Myc, which localizes TAT-merlin isoform 1 to the plasma membrane (E). (E) Particulate likely represents clumps of TAT-merlin that did not enter cells.

contain such low levels of merlin that it is not detectable on Western blots. Normal human Schwann cells treated with TAT-merlin for 5 h and then washed contained TAT-merlin (detected by anti-Myc) on Western blotting (Fig. 2C, lane 2). When 5 h of exposure was followed by a 16-h washout (Fig. 2C, lane 3), little Myc-tagged merlin was detected. Schwannoma cells were incubated with TAT-merlin and then washed, fixed, and stained with anti-Myc antibody (Fig. 2E). After 5 h of incubation, merlin protein was detected at the plasma membrane, as anticipated (10, 38, 39, 42). All cells were labeled by anti-Myc, indicating merlin introduction. Since Myc staining was not detectable with shorter incubations, subsequent experiments used 5 h of incubation in TAT proteins.

TAT-merlin isoform 1 reverses cytoskeletal defects in schwannoma cells. We tested the ability of TAT-merlin isoform 1 to inhibit aberrant ruffling and cell spreading phenotypes of schwannoma cells. Previous experiments with TAT-linked proteins used 10 to 140 nM TAT fusion protein (28). As no biochemical assay is available for merlin function, this range of concentrations was used in an attempt to reverse schwannoma cell defects. Cells were treated with TAT-merlin for 5 h, removed from dishes with trypsin, and then plated for ruffling or spreading assays. In a dose-dependent manner, treatment with TAT-merlin isoform 1 dramatically reduced the ruffling

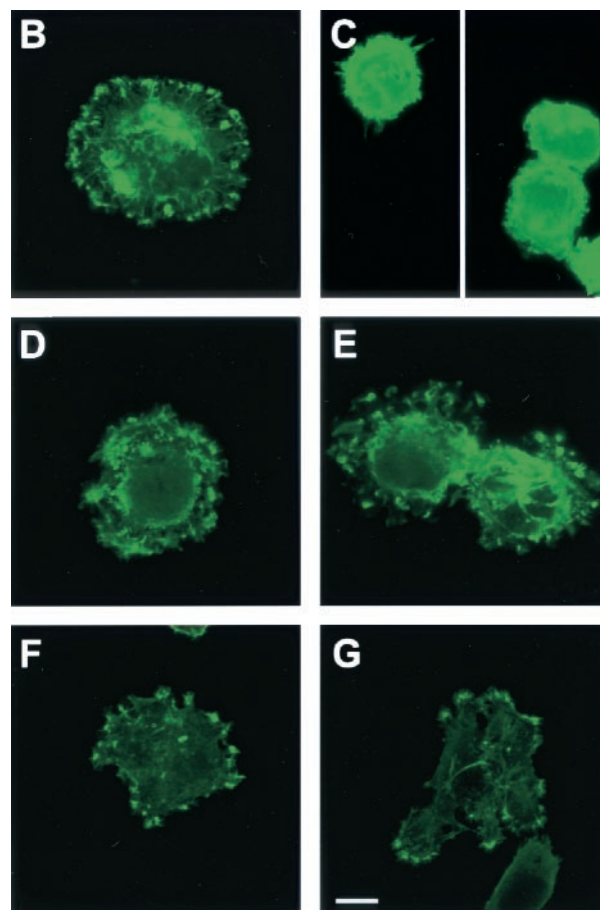
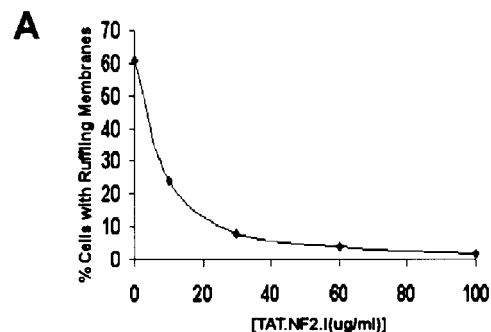


FIG. 3. TAT-merlin isoform 1 specifically reverses schwannoma cell membrane ruffling. (A) Schwannoma cells were exposed to the designated concentrations of purified TAT-merlin. Cells were then replated onto laminin-coated coverslips and exposed to serum. Cells were stained, and the percentage of S100β-positive cells with ruffling membranes was quantitated. (B to G) Alexa-phalloidin-labeled cells are shown. In each case, schwannoma cells were treated with 60 µg of designated protein per ml. (B) No protein was added. Schwannoma cells were exposed to TAT-merlin 1 (C), merlin 1 (no TAT) (D), TAT-merlin isoform 2 (E), TAT-β-galactosidase (F), and TAT-L64P merlin isoform 1 (G). Bar, 10 µm.

phenotype characteristic of *NF2*-deficient cells (Fig. 3A), and similar results were observed in three different tumor cell preparations (Fig. 4B). TAT-merlin isoform 1-treated cells assumed a rounded morphology like that of normal human Schwann cells (Fig. 3B and 3C).

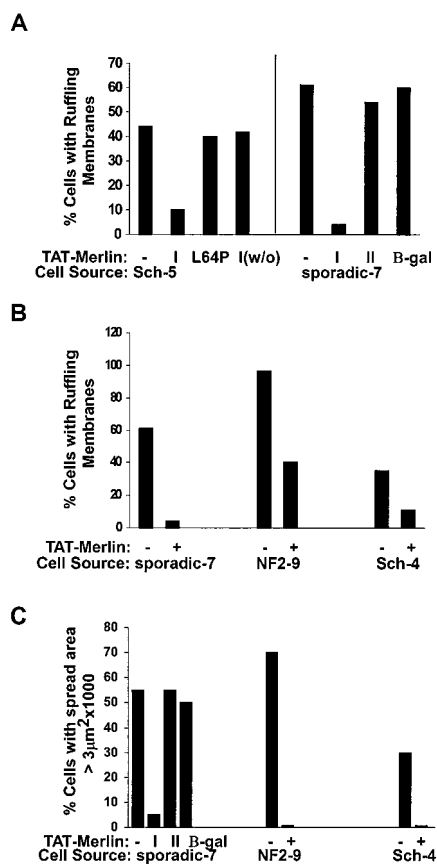


FIG. 4. TAT-merlin isoform 1 specifically reverses the F-actin cytoskeletal defects in schwannoma cells: quantitation. (A and B) TAT-merlin isoform 1 was added to cells from the tumor type designated under the *x* axis. Cells were replated onto laminin in the presence of serum. The percentage of cells with membrane ruffles was measured as for Fig. 1 and 3. (A) Left of the vertical line, TAT-merlin isoform 1 (I) but not TAT-merlin isoform 1 with a mutation (L64P) reverses schwannoma cell membrane ruffling. The effects of TAT-merlin isoform 1 were reversed when cells were treated with TAT-merlin 1 for 5 h and then exposed overnight to medium without TAT-merlin isoform 1 (1w/o). To the right of the vertical line, membrane ruffling was inhibited by TAT-merlin isoform 1 (I) but not TAT-merlin isoform 2 (II) or TAT- β -galactosidase (β -gal). (C) From each tumor type designated under the *x* axis, cells were exposed to 60 μ g of TAT-merlin isoform 1 and then washed, replated, and stained as for panel A, and their spread areas were measured.

To confirm the specificity of these results, control experiments were carried out. To exclude the possibility that merlin protein could act outside cells, merlin without a TAT tag (Fig. 3D) was added to cells but did not correct the ruffling defect. TAT- β -galactosidase also failed to correct schwannoma cell ruffling (Fig. 3F). Another control was to add TAT-merlin to schwannoma cells for 5 h, change the medium, and incubate for 16 h without TAT-merlin. After washout, schwannoma cells showed ruffling membranes similar to untreated schwannoma cells (Fig. 4A). Furthermore, merlin carrying a missense mutation, L64P (13), did not reverse the phenotype (Fig. 3G and 4A). Merlin has two isoforms resulting from alternative splicing (1). Merlin isoform 1 but not isoform 2 suppressed ruffling and cell size defects (Fig. 3C, 3E, and 4A).

We previously showed that schwannoma cells ruffle on con-

tact with fibronectin and collagen as well as on laminin. Because laminin and fibronectin but not collagen are enriched in schwannomas, we tested if the reversal occurs on fibronectin. TAT-merlin isoform 1 but not TAT-merlin L64P inhibited ruffling of schwannoma cells plated onto fibronectin (not shown). The percentages of inhibition of ruffling on fibronectin and laminin were identical.

Coverslips containing cells exposed to TAT-merlin isoform 1 had significantly fewer schwannoma cells than did the untreated cells. Thirty minutes after plating, the number of TAT-merlin isoform 1-treated cells adhering to the coverslips decreased in a dose-dependent manner; at 60 μ g of TAT-merlin isoform 1 per ml in three experiments with cells from three different schwannomas, 34, 6, and 21% of cells were adherent (not shown) compared to untreated controls. Lack of attachment was not observed when cells were treated with TAT-merlin isoform 2 or when NHSCs were treated with TAT-merlin isoform 1 at 60 μ g/ml (not shown). When TAT-merlin-treated schwannoma cells were counted 3 h after plating, 72% of cells were attached (not shown). Thus, concurrent with loss of ruffling, introduction of merlin causes transient inhibition of cell attachment.

Three hours after plating, most TAT-merlin isoform 1-treated schwannoma cells had surface areas smaller than those of the untreated controls and comparable to those of NHSCs. Figure 4C shows size measurements on cells from a sporadic schwannoma, a schwannoma from an NF2 patient, and a schwannoma from a schwannomatosis patient. In each case, exposure to TAT-merlin isoform 1 but not TAT-merlin isoform 2 dramatically reduced cell size.

To determine the specificity of this approach, normal human Schwann cells were treated with TAT-merlin isoform 1, TAT-merlin L64P, or merlin with no TAT. No changes in cell morphology were observed (not shown). No cells with ruffling membranes or increase in cell size were detected (not shown). Furthermore, the number of attached cells was not significantly different in each group (number of attached cells: no TAT-merlin, 855 cells/coverslip; TAT-merlin L64P, 836 cells/coverslip; TAT-merlin isoform 1, 968 cells/coverslip).

DISCUSSION

We have established that NF2-deficient schwannoma cells, whether isolated from schwannomatosis patients, NF2 patients, or sporadic schwannomas, exhibit cytoskeletal abnormalities manifested by membrane ruffling and large surface areas. The effects are specific to schwannoma cells, as they are not found in Schwann cells from normal human nerve or neurofibromas. Thus, whether the NF2 mutation is acquired subsequent to inherited mutation at the schwannomatosis locus, inherited mutation at NF2, or sporadically, schwannoma cells have a common cytoskeletal phenotype.

Schwannoma cells, like normal Schwann cells, express matrix-binding integrins α 2 β 1 and α 6 β 1 (34). Within schwannomas, cells are surrounded by a laminin- and fibronectin-rich matrix (5). Cells bind to the matrix via cell surface receptors, including a β 1 integrin, with which merlin coprecipitates (30). Our previous data showed ruffling and spreading defects when schwannoma cells contact laminin and fibronectin (32). Here we show that schwannoma cells of all three classes ruffle on

contact with laminin. TAT-merlin reversed ruffling on both laminin and fibronectin.

Integrin activation stimulates Rho and Rac GTPases, to which ERM proteins have been directly linked (22, 41). Shaw et al. placed merlin in the Rac-JNK signaling pathway and showed that merlin is a substrate for Rac-mediated phosphorylation (43). They proposed a model in which active, dephosphorylated merlin attenuates Rac signals and inactive, phosphorylated merlin potentiates Rac signaling. Our results in schwannoma cells, which lack merlin, are consistent with this model, as they have increased ruffling that can be inhibited by dominant negative Rac (32). Hyperactivation of Rac may result from elevated Rac activation, decreased Rac inactivation, or merlin-mediated control of Rac localization. The lack of biochemical quantities of schwannoma cells precludes differentiation among these possibilities at this time.

In addition to its role in actin cytoskeletal organization (33), Rac signaling can enhance cell proliferation stimulated by adhesion to fibronectin (26). Overexpression of merlin increased cell growth in confluent cells, and merlin and the haluronic acid receptor CD44 form a molecular switch specifying cell growth arrest or proliferation (27).

We chose to focus our analysis on schwannoma cell cytoskeletal defects for several reasons. First, cell proliferation is elevated in cells from some but not all schwannomas, while cytoskeletal defects are present in cells from all tumors (32). Second, cytoskeletal alterations may be linked to changes in cell growth and ultimately tumor formation. Altered schwannoma cell-matrix interactions are likely to be relevant to cell growth and the integrity of the cytoskeleton.

The percentage of schwannoma cells exhibiting membrane ruffling and increased cell size varies from tumor to tumor. There seem to be two populations of Schwann cells per tumor, one that exhibits cytoskeletal abnormalities and one that does not, because the percentage of cells with abnormal actin cytoskeleton does not change with increased passage number. We cannot exclude the possibility that phenotypic differences reflect normal Schwann cells within the sample through contamination from normal nerve during tumor resection. However, genetic analysis failed to reveal large amounts of contaminating wild-type allele, and several tumors analyzed were removed via open craniotomy, making this unlikely (see the discussion in reference 45). The reproducible heterogeneity among cells from individual tumors might also reflect the two histological areas in schwannomas, Antoni A and B (7), with cells from these regions having different phenotypes. A related possibility is a predisposition for a second genetic event(s) occurring in some but not all cells.

The severity of individual patients' disease was not obviously correlated with the extent of membrane ruffling or cell size. For example, two tumors from a single patient with severe disease (NF2-5 and NF2-6) had high ruffling membranes but one had 35% and the other 100% large cells. Two other patients, NF2-8 and NF2-1, had very similar severe disease, but 40 and 35% of their cells were ruffled.

Also, there was no correlation between the percentage of cells with aberrant ruffling and those that had large cell size in a given tumor cell strain, and ruffling was observed independent of cell size. This leaves open the possibility of different genetic or epigenetic changes in addition to *NF2* mutation

underlying the two phenotypes. The idea that an additional mutation(s) secondary to *NF2* mutation is necessary for formation of schwannomas is supported by evidence in the *NF2* conditional knockout mouse. In these mice, schwannomas occur at low frequency, although most Schwann cells are predicted to have lost *NF2* function (9). If mutations occur at loci other than *NF2* in human schwannoma formation, they remain unidentified.

We hypothesized that if lack of merlin causes abnormal cytoskeletal organization, then adding merlin back to schwannoma cells would reverse the phenotype. Initiating mutations, when reversed, are sufficient to control tumor growth even late in tumorigenesis (4). When treated with TAT-merlin isoform 1, schwannoma cells exhibited a decrease in membrane ruffling and had a smaller surface area. There are several reasons to believe that this effect was specific. First, this effect was not mimicked by TAT- β -galactosidase or by merlin without a TAT sequence. Second, this effect was both dose and time dependent. Although the mechanism by which TAT fusion proteins transduce cells is not known, TAT protein effects are concentration dependent (28). Third, the effects of TAT-merlin were reversible. Reversibility could occur if TAT-merlin inside cells becomes degraded and/or if TAT-merlin uses the TAT transporter mechanism to exit cells when the extracellular TAT-merlin concentration is lower than that inside the cells. In either case, the reversibility argues that the ruffling phenotype occurs only when TAT-merlin isoform I was present inside the cells. Finally, similar levels of TAT-merlin isoform 1 did not affect attachment or the actin cytoskeleton of normal human Schwann cells.

TAT-merlin isoform 2 did not reverse the cytoskeletal defects in schwannoma cells although the alternatively spliced *NF2* mRNA is present in Schwann cells (1, 24). Similarly, only merlin isoform 1 complements growth defects in transformed cell lines (44). The merlin fusion proteins used here were tagged at their C and N termini. These tags did not compromise the ability of TAT-merlin isoform 1 protein to reverse the cytoskeletal phenotypes, in spite of evidence that missense mutations that impair merlin folding inhibit its ability to suppress growth and cell spreading (14). Our results are consistent with those of Shaw et al., who showed that a C-terminally Myc-tagged merlin isoform 1 inhibits phosphorylation of c-jun N-terminal kinase downstream of Rac as effectively as or better than untagged merlin (43). However, we cannot rule out the possibility that untagged amino and/or carboxy termini are necessary for TAT-merlin isoform 2 to function in Schwann cells.

Previous studies utilizing merlin over- and underexpression and merlin missense mutants all reported loss of cell adhesion in cell lines (13, 17, 46). Interestingly, the introduction of TAT-merlin caused a transient reduction in attachment to laminin, concomitant with decreased membrane ruffling, of schwannoma cells but not normal human Schwann cells. Cell type-specific merlin usage or relative merlin concentration could explain these varied results. TAT-merlin induced attenuation of cell-substrate interaction and of ruffling are likely related phenotypes, consistent with the view that merlin acts as a tumor suppressor by regulating cell-matrix interaction.

We conclude that merlin isoform 1 is sufficient to reverse the abnormal F-actin cytoskeletal phenotypes exhibited by *NF2*-

deficient tumor cells. TAT-linked proteins are taken up into the nervous system (40), so in view of the specificity of TAT-merlin for schwannoma cells, it could in principle be used therapeutically. Our experiments therefore lay the foundation for epigenetic complementation studies in NF2 mouse models and for treating NF2-deficient tumors using TAT-merlin, which may, in the future, be used alone or in conjunction with other therapies.

ACKNOWLEDGMENTS

We thank S. Dowdy and coworkers (Washington University, St. Louis, Mo.) for constructs and advice concerning the TAT system; Patrick Wood, Les Olsen, and the University of Miami Organ Procurement Team for providing human nerves; and Mark Marchionni (Cambridge Neuroscience) for rhGGF2. University of Cincinnati GCRG MO1RR 08084 and the Midwest Human Tissue Acquisition Network (Columbus, Ohio) provided some specimens. The IRBs of the University of Cincinnati and Massachusetts General Hospital approved this work. We thank all patients and families who generously donated tissue.

This work was supported by NIH CA 78524 to W.I. and N.R., NS35878 to M.M., and FS CA 80385 to A.-M.B.

REFERENCES

- Bianchi, A., T. Hara, V. Ramesh, J. Gao, A. Klein-Szanto, F. Morin, A. Menon, J. Trofatter, J. Gusella, et al. 1994. Mutations in transcript isoforms of the neurofibromatosis 2 gene in multiple human tumour types. *Nat. Genet.* **6**:185–192.
- Bretscher, A., D. Chambers, R. Nguyen, and D. Reczek. 2000. ERM-Merlin and EBP50 protein families in plasma membrane organization and function. *Annu. Rev. Cell. Dev. Biol.* **16**:113–143.
- Bruder, C. E., C. Hirvela, I. Tapia-Paez, I. Fransson, R. Segraves, G. Hamilton, Z. Z. Zhang, D. G. Evans, A. J. Wallace, et al. 2001. High resolution deletion analysis of constitutional DNA from neurofibromatosis type 2 (NF2) patients using microarray-CGH. *Hum. Mol. Genet.* **10**:271–282.
- Chin, L., A. Tam, J. Pomerantz, M. Wong, J. Holash, N. Bardeesy, Q. Shen, R. O'Hagan, J. Pantginis, et al. 1999. Essential role for oncogenic Ras in tumour maintenance. *Nature* **400**:468–472.
- d'Ardenne, A. J., P. Kirkpatrick, and B. C. Sykes. 1984. Distribution of laminin, fibronectin, and interstitial collagen type III in soft tissue tumours. *J. Clin. Pathol.* **37**:895–904.
- den Bakker, M. A., P. H. Riegman, A. P. Suurmeijer, C. J. Vissers, M. Sainio, O. Carpen, and E. C. Zwarthoff. 2000. Evidence for a cytoskeleton attachment domain at the N terminus of the NF2 protein. *J. Neurosci. Res.* **62**:764–771.
- Erlanson, R. A., and J. M. Woodruff. 1982. Peripheral nerve sheath tumors: an electron microscopic study of 43 cases. *Cancer* **49**:273–287.
- Evans, D. G., L. Trueman, A. Wallace, S. Collins, and T. Strachan. 1998. Genotype/phenotype correlations in type 2 neurofibromatosis (NF2): evidence for more severe disease associated with truncating mutations. *J. Med. Genet.* **35**:450–455.
- Giovannini, M., E. Robanus-Maandag, M. van der Valk, M. Niwa-Kawakita, V. Abramowski, L. Goutebroze, J. M. Woodruff, A. Berns, and G. Thomas. 2000. Conditional biallelic NF2 mutation in the mouse promotes manifestations of human neurofibromatosis type 2. *Genes Dev.* **14**:1617–1630.
- Gonzalez-Agosti, C., L. Xu, D. Pinney, R. Beauchamp, W. Hobbs, J. Gusella, and V. Ramesh. 1996. The merlin tumor suppressor localizes preferentially in membrane ruffles. *Oncogene* **13**:1239–1247.
- Gronholm, M., M. Sainio, F. Zhao, L. Heiska, A. Vaheri, and O. Carpen. 1999. Homotypic and heterotypic interaction of the neurofibromatosis 2 tumor suppressor protein merlin and the ERM protein ezrin. *J. Cell Sci.* **112**:895–904.
- Gutmann, D. H., A. Aylsworth, J. C. Carey, B. Korf, J. Marks, R. E. Pyeritz, A. Rubenstein, and D. Viskochil. 1997. The diagnostic evaluation and multidisciplinary management of neurofibromatosis 1 and neurofibromatosis 2. *JAMA* **278**:51–57.
- Gutmann, D. H., L. Sherman, L. Sefter, C. Haipek, K. Hoang Lu, and M. Hendrix. 1999. Increased expression of the NF2 tumor suppressor gene product, merlin, impairs cell motility, adhesion and spreading. *Hum. Mol. Genet.* **8**:267–275.
- Gutmann, D. H., A. C. Hirbe, and C. A. Haipek. 2001. Functional analysis of neurofibromatosis 2 (NF2) missense mutations. *Hum. Mol. Genet.* **10**:1519–1529.
- Huang, L., E. Ichimaru, K. Pestonjamas, X. Cui, H. Nakamura, G. Y. Lo, F. I. Lin, E. J. Luna, and H. Furthmayr. 1998. Merlin differs from moesin in binding to F-actin and in its intra- and intermolecular interactions. *Biochem. Biophys. Res. Commun.* **248**:548–553.
- Hung, G., R. Faudoa, X. Li, Z. Xeu, D. E. Brackmann, W. Hitzelberg, E. Saleh, F. Lee, D. H. Gutmann, et al. 1999. Establishment of primary vestibular schwannoma cultures from neurofibromatosis type-2 patients. *Int. J. Oncol.* **14**:409–415.
- Huynh, D. P., and S. M. Pulst. 1996. Neurofibromatosis 2 antisense oligodeoxynucleotides induce reversible inhibition of schwannomin synthesis and cell adhesion in STS26T and T98G cells. *Oncogene* **13**:73–84.
- Irving, R. M., T. Harada, D. A. Moffat, D. G. Hardy, J. L. Whittaker, J. H. Xuereb, and E. R. Maher. 1997. Somatic neurofibromatosis type 2 gene mutations and growth characteristics in vestibular schwannoma. *Am. J. Otol.* **18**:754–760.
- Jacoby, L. B., D. Jones, K. Davis, D. Kronn, M. P. Short, J. Gusella, and M. MacCollin. 1997. Molecular analysis of the NF2 tumor-suppressor gene in schwannomatosis. *Am. J. Hum. Genet.* **61**:1293–1302.
- Johnson, M. D., A. D. Glick, and B. W. Davis. 1988. Immunohistochemical evaluation of Leu-7, myelin basic-protein, S100-protein, glial-fibrillary acidic-protein, and LN3 immunoreactivity in nerve sheath tumors and sarcomas. *Arch. Pathol. Lab. Med.* **112**:155–160.
- Kawahara, E., Y. Oda, A. Ooi, S. Katsuda, I. Nakanishi, and S. Umeda. 1988. Expression of glial fibrillary acidic protein (GFAP) in peripheral nerve sheath tumors. *Am. J. Surg. Pathol.* **12**:115–120.
- Maeda, M., T. Matsui, M. Imamura, S. Tsukita, and S. Tsukita. 1999. Expression level, subcellular distribution and rho-GDI binding affinity of merlin in comparison with ezrin/radixin/moesin proteins. *Oncogene* **18**:4788–4797.
- Marchionni, M. A., A. D. Goodearl, M. S. Chen, O. Birmingham-McDonogh, C. Kirk, M. Hendricks, F. Danehy, D. Misumi, J. Sudhalter, et al. 1993. Glial growth factors are alternatively spliced erbB2 ligands expressed in the nervous system. *Nature* **362**:312–318.
- Meng, J. J., D. J. Lowrie, H. Sun, E. Dorsey, P. D. Pelton, A.-M. Bashour, J. Groden, N. Ratner, and W. Ip. 2000. Interaction between two isoforms of the NF2 tumor suppressor protein, merlin, and between merlin and ezrin, suggests modulation of ERM proteins by merlin. *J. Neurosci. Res.* **62**:491–502.
- Merel, P., K. Haong-Xuan, M. Sanson, A. Moreau-Aubry, E. K. Bijlsma, C. Lazaro, J. P. Moisan, F. Resche, I. Nishisho, et al. 1995. Predominant occurrence of somatic mutations of the NF2 gene in meningiomas and schwannomas. *Genes Chromosomes Cancer* **13**:211–216.
- Mettouchi, A., S. Klein, W. Guo, M. Lopez-Lago, E. Lemichez, J. Westwick, and F. Giancotti. 2001. Integrin-specific activation of Rac controls progression through the G₁ phase of the cell cycle. *Mol. Cell* **8**:115–127.
- Morrison, H., L. Sherman, J. Legg, F. Banine, C. Isacke, C. A. Haipek, D. H. Gutmann, H. Ponta, and P. Herrlich. 2001. The NF2 tumor suppressor gene product, merlin, mediates contact inhibition of growth through interactions with CD44. *Genes Dev.* **15**:968–980.
- Nagahara, H., A. M. Vocero-Akbani, E. L. Snyder, A. Ho, D. G. Latham, N. A. Lissy, M. Becker-Hapak, S. A. Ezhevsky, and S. F. Dowdy. 1998. Transduction of full-length TAT fusion proteins into mammalian cells: TAT-p27Kip1 induces cell migration. *Nat. Med.* **4**:1449–1452.
- Nguyen, R., D. Reczek, and A. Bretscher. 2001. Hierarchy of merlin and ezrin N- and C-terminal domain interactions in homo- and heterotypic associations and their relationship to binding of scaffolding proteins EBP50 and E3KARP. *J. Biol. Chem.* **276**:7621–7629.
- Obrenski, V. J., A. M. Hall, and C. Fernandez-Valle. 1998. Merlin, the neurofibromatosis type 2 gene product, and beta1 integrin associate in isolated and differentiating Schwann cells. *J. Neurobiol.* **37**:487–501.
- Parry, D. M., M. M. MacCollin, M. I. Kaiser-Kupfer, K. Pulaski, H. S. Nicholson, M. Bolesta, R. Eldridge, and J. F. Gusella. 1996. Germ-line mutations in the neurofibromatosis 2 gene: correlations with disease severity and retinal abnormalities. *Am. J. Hum. Genet.* **59**:529–539.
- Pelton, P. D., T. A. Rizvi, L. Sherman, M. A. Marchionni, P. Wood, R. A. Friedman, and N. Ratner. 1998. Ruffling membrane, stress fiber, cell spreading and proliferation abnormalities in human Schwann cells. *Oncogene* **17**:2195–2209.
- Ridley, A. J., H. F. Paterson, C. L. Johnston, D. Diekmann, and A. Hall. 1992. The small GTP-binding protein Rac regulates growth factor-induced membrane ruffling. *Cell* **70**:401–410.
- Roche, P. H., D. Figarella-Branger, L. Daniel, N. Bianco, W. Pellet, and J. F. Pellissier. 1997. Expression of cell adhesion molecules in normal nerves, chronic axonal neuropathies and Schwann cell tumors. *J. Neurol. Sci.* **151**:127–133.
- Rosenbaum, C., L. Kluwe, V. F. Mautner, R. E. Friedrich, H. W. Muller, and C. O. Hanemann. 1998. Isolation and characterization of Schwann cells from neurofibromatosis type 2 patients. *Neurobiol. Dis.* **5**:55–64.
- Rouleau, G. A., P. Merel, M. Lutchman, M. Sanson, J. Zucman, C. Marinneau, K. Hoang-Xuan, S. Demczuk, C. Desmaze, B. Plougastel, et al. 1993. Alteration in a new gene encoding a putative membrane-organizing protein causes neuro-fibromatosis type 2. *Nature* **363**:515–521.
- Rutledge, M. H., A. A. Andermann, C. M. Phelan, J. O. Claudio, F. Y. Han, N. Chretien, S. Ranganatnam, M. MacCollin, P. Short, et al. 1996. Type of mutation in the neurofibromatosis type 2 gene (NF2) frequently determines severity of disease. *Am. J. Hum. Genet.* **59**:331–342.
- Sainio, M., F. Zhao, L. Heiska, O. Turunen, M. den Bakker, E. Zwarthoff, M. Lutchman, G. A. Rouleau, J. Jaaskelainen, et al. 1997. Neurofibromatosis 2

- tumor suppressor protein colocalizes with ezrin and CD44 and associates with actin-containing cytoskeleton. *J. Cell Sci.* **110**:2249–2260.
39. **Scherer, S. S., and D. H. Gutmann.** 1996. Expression of the neurofibromatosis 2 tumor suppressor gene product, merlin, in Schwann cells. *J. Neurosci. Res.* **46**:595–605.
 40. **Schwarze, S. R., K. Hruska, and S. F. Dowdy.** 2000. Protein transduction: unrestricted delivery into all cells? *Trends Cell Biol.* **10**:290–295.
 41. **Shaw, R. J., M. Henry, F. Solomon, and T. Jacks.** 1998. RhoA-dependent phosphorylation and relocalization of ERM proteins into apical membrane/actin protrusions in fibroblasts. *Mol. Biol. Cell* **9**:403–419.
 42. **Shaw, R. J., A. I. McClatchey, and T. Jacks.** 1998. Localization and functional domains of the neurofibromatosis type II tumor suppressor, merlin. *Cell Growth Differ.* **9**:287–296.
 43. **Shaw, R. J., J. G. Paez, M. Curto, A. Yaktine, W. M. Pruitt, I. Saotome, J. P. O'Brian, V. Gupta, N. Ratner, C. J. Der T. Jacks, and A. I. McClatchey.** 2001. The *NF2* tumor suppressor, merlin, functions in Rac-dependent signaling. *Dev. Cell* **1**:63–72.
 44. **Sherman, L., H-M. Xu, R. T. Geist, S. Saporito-Irwin, N. Howells, P. Ponta, P. Herrlich, and D. Gutmann.** 1997. Interdomain binding mediates tumor growth suppression by the NF2 gene product. *Oncogene* **15**:2505–2509.
 45. **Stemmer-Rachamimov, A. O., L. Xu, C. Gonzalez-Agosti, J. A. Burwick, D. Pinney, R. Beauchamp, L. B. Jacoby, J. F. Gusella, V. Ramesh, et al.** 1997. Universal absence of merlin, but not other ERM family members, in schwannomas. *Am. J. Pathol.* **151**:1649–1654.
 46. **Stokowski, R. P., and D. R. Cox.** 2000. Functional analysis of the neurofibromatosis type 2 protein by means of disease-causing point mutations. *Am. J. Hum. Genet.* **66**:873–891.
 47. **Trofatter, J. A., M. M. MacCollin, J. L. Rutter, J. R. Murrell, M. P. Duyao, D. M. Parry, R. Eldridge, N. Kley, A. G. Menon, K. Pulaski, et al.** 1993. A novel moesin-, ezrin-, radixin-like gene is a candidate for the neurofibromatosis 2 tumor suppressor. *Cell* **72**:791–800.
 48. **Xu, H-M., and D. H. Gutmann.** 1998. Merlin differentially associates with the microtubule and actin cytoskeleton. *J. Neurosci. Res.* **51**:403–415.